ELSEVIER

Physica A 217 (1995) 373–392

PHYSICA A

Phase diagram of a model of self-organizing hierarchies

Eric Bonabeau[a, b, *], Guy Theraulaz[c], Jean-Louis Deneubourg[d]

[a] *CNET Lannion B–RIO/TNT, route de Trégastel, 22301 Lannion Cédex, France*
[b] *Laboratoire de Physique des Solides, Université Paris-Sud, 91405 Orsay Cédex, France*
[c] *CNRS–URA 1837, Laboratoire d'Ethologie et de Psychologie Animale, Université Paul Sabatier, 118 route de Narbonne, 31062 Toulouse, France*
[d] *Unit of Theoretical Behavioral Ecology, Service de Chimie-Physique, CP 231, Université Libre de Bruxelles, Boulevard du triomphe, 1050 Bruxelles, Belgium*

Received 14 February 1995

Abstract

We introduce a simple model of self-organizing hierarchies in animal societies which relies on a basic positive feedback mechanism reinforcing the ability of a given individual to win or lose in a hierarchical interaction, depending on how many times it won or lost in previous interactions. If a forgetting strength is included, which determines the rate at which events in the past are forgotten and no longer influence the force of an individual, subcritical or supercritical bifurcations in the formation of the hierarchical structure are observed as the density ρ of individuals is varied. The nature of the transition is shown to depend on a parameter η, analogous to the inverse of a temperature, defining the amount of determinism in the outcomes of the fights. We therefore observe a dynamical tricritical point in the ρ–η plane.

1. Introduction and model

The existence of a non-equilibrium, dynamical, tricritical point, implying a crossover from a subcritical to a supercritical bifurcation, has been shown experimentally in the Couette–Taylor hydrodynamic instability [1], or in directional solidification [2]. In the latter case, the crossover in the Mullins–Sekerka planar-cellular instability had previously been predicted theoretically [3]. Such a modification in the nature of the observed transition can often be traced back to the normal form or the Landau equation describing the evolution of the order parameter or of a small perturbation. The canonical example is given by [4]

$$\frac{dM}{dt} = (\rho - \rho_c)M - \alpha\frac{M^3}{M_0^2} + M^5, \tag{1}$$

* Corresponding author.

0378-4371/95/$09.50
SSDI 0378-4371(95)00064-X

where M is the order parameter, ρ is the control parameter, M_0 sets the scale for M above threshold and α is the parameter upon which the nature of the bifurcation relies: $\alpha > 0$ yields a critical bifurcation and $\alpha < 0$ yields a subcritical bifurcation; $\alpha = 0$ is a special case which depends on higher-order terms in (1). Examples of this behavior are not restricted to physical examples. Some biological models exhibit this crossover and have a clear predictive power: see e.g. the model of parturition of Sornette et al. [5] or the model of self-organized foraging of Millonas [6]. We propose in this paper to study a biologically motivated model of self-organizing hierarchies in animal societies exhibiting this crossover. We expect our work not to be just one more example – although analytically solvable – falling in the class of normal form (1); we believe that it can also provide new insights into biological phenomena from a perspective which is more familiar to physicists. The rest of the paper is organized as follows: we first introduce the model and its motivation; in Section 2, we report results of Monte Carlo simulations, and introduce a mean-field approach to these simulations in Section 3, where our results concerning the mean-field theory are presented; we prove these results exactly for 2 individuals in Section 4 and give heuristic arguments for larger populations in Section 5.

The emergence of hierarchies in animal groups, colonies and societies is a phenomenon which has attracted a lot of attention for a long time [7]. Hierarchical behavior has been described in chickens [8], cows [9], ponies [10] and social insects, especially in wasps [11,12] and ants [13]. Van Honk and Hogeweg [14] proposed a model based on experimental observations of bumble bees *Bombus terrestris*, assuming that a simple positive feedback mechanism could explain the formation of a hierarchy: the more an individual wins, the more likely it is to win in future fights. The model we present here is based on a similar hypothesis.

If two individual i and j start a hierarchical interaction, the outcome of the fight is assumed to be probabilistic: individual i wins with a probability given by $Q_{ij}^{+} = 1/(1 + e^{-\eta\Delta_{ji}})$, with $\Delta_{ij} = F_i - F_j$, where F_i is a quantity that we call force, increased by a constant value (δ^+) in case of victory and decreased by a constant value (δ^-) in case of defeat. One can interpret this force as an indicator of the physiological state of the individual (including, e.g. in some social insects such as wasps, the activity of the corpora allata (CA) or the level of juvenile hormone (JH) in the hemolymph: CA activity and JH level have been found to increase with hierarchical rank [15]). We shall assume for simplicity that $\delta^+ = \delta^- = 1$, so that F_i is just proportional to the number of times the individual has been successful minus the number of times it has been dominated. The probability for i to lose is equal to the probability for j to win: $Q_{ij}^{-} = Q_{ji}^{+} = 1/(1 + e^{-\eta\Delta_{ij}}) = 1 - Q_{ij}^{+}$. This rule is analogous to the heat bath of Ising spins, where the up direction fights against the down direction; the interactions here are of an "antiferromagnetic" nature, i.e. relative individual differences between spins are favoured.

It is natural to introduce forgetting, i.e. a relaxation to 0 of F_i in the absence of any external stimulation. It has indeed been observed that e.g. an individual cockroach withdrawn from the hierarchical game for a certain amount of time does not recover

its previous rank [16]. If we assume that individuals move randomly in a space where they can encounter other individuals, it is in fact the ratio between the probability of interaction (= the probability to meet another individual at the current location) and the forgetting rate which is relevant. For instance, a densely populated region should correspond to a higher probability of interaction than sparsely distributed individuals: therefore, there is a connection between the formation of hierarchies and the density of population. It is also tempting to draw a parallel with human social organizations, where it is known that the density of population is tightly coupled with the existence of a hierarchical structure: the history of sociology shows us that low density zones (such as rural regions) are loosely hierarchical, while towns (ancient cities such as Babylonia, but also modern cities) exhibit a strong hierarchical organization. Depending on the degree of determinism in the outcomes of "hierarchical interactions", we predict the smooth or abrupt appearance of a hierarchical structure upon varying the density of population. Such a connection may be too simplistic (all the more as it is experimentally difficult to validate), since a hierarchical structure is certainly the aggregate result of many interacting factors. We believe, however, that more sophisticated versions of the present model, e.g. involving recognition between individuals, could apply more closely to human organizations. Finally, let us note that the simplest possible application of such a model to a human organization would be the rating of tennis or chess players! In effect, the forgetting rate, i.e. the "spontaneous decay rate" of a player's rank, must be adjusted so as to permit the existence of a well-defined hierarchy. Can we imagine tennis without a number 1?

2. Monte Carlo simulations

In order to visualize the transition from a non-hierarchical to a hierarchical behavior when the density of individuals is increased, we have run Monte Carlo simulations of N individuals performing a random walk on a 2D square lattice: at each discrete time step, all individuals arrive at a site where there may be another individual (there are 0, 1, or 2 individuals at any particular site); then a fight takes place and the probabilistic outcome is given by the above mentioned sigmoid function Q, and the forces of both individuals are incremented (the winner) or decremented (the loser) by 1. The forces of all individuals relax towards 0 at each time step as follows: $F \to F - \mu \tanh(F)$, where μ is a small parameter determining the forgetting rate. Both the winner and the loser continue their random walks after the fight.

The instantaneous dynamics of the hierarchical profile can be characterized by the set $\{\langle P_i \rangle\}$ where $\langle P_i \rangle = 1/(N-1) \sum_{j=1/j \neq i}^{N} [1/(1 + e^{-\eta(F_i - F_j)})]$ denotes the instantaneous probability that individual i wins in a random fight. The "statics" is well described by a biologically relevant quantity $X_i = D_i/(D_i + S_i)$ where D_i (resp. S_i) is the number of fights won (resp. lost) by individual i: X gives a good image of the overall probability integrated over time of an individual to win against another randomly selected individual. This particular index was used in the pioneering work

of Pardi [11] under the name of "dominance index". Note that X does not vary if no interactions takes place. Therefore, when an individual moves for a long time without interacting, its force relaxes to 0, but its dominance index X remains at the value it was set after the last encounter: $\langle P_i \rangle$ then gives a better dynamic picture of the real instantaneous dominance index, but both are asymptotically equivalent. Moreover, it is, as we shall see, more convenient to use X in the mean-field approach presented next, and X then gives the same information as $\langle P_i \rangle$ since in the mean-field theory interactions take place *at every time step.* Another advantage of X_i is that it is experimentally accessible, contrary to $\langle P_i \rangle$, and thus our results in terms of X can be confronted with biological data.

We observe that no non-uniform hierarchical profile gets established if the population density ρ is too low: $\forall i, X_i = \frac{1}{2}$, even after a long time. It simply stems from the fact that the force of every individual has time to relax to 0 between two successive encounters. See Figs. 1–4, where the time evolutions of 15 randomly chosen $\langle P_i \rangle$'s are represented for different values of ρ (the number N of individuals is 50 000 in all cases, the linear size L of the lattice is varied from 300 to 1000: $\rho = N/L \times L$). The values used in these figures are $\eta = 5$ and $\mu = 0.1$. When ρ lies below a value ρ_c (≈ 0.1 in the present case), no stable asymptotic profile can be reached: the evolution of $\langle P_i \rangle$ (see Fig. 4) is erratic, and the temporal average of X_i is equal to 0.5, i.e. a flat profile. Above ρ_c, a non-uniform asymptotic profile ($\exists i \langle \langle P_i \rangle \rangle \neq 0.5$) emerges and all $\langle P_i \rangle$'s become stable after a very short time and rapidly reach their asymptotic values, which are all

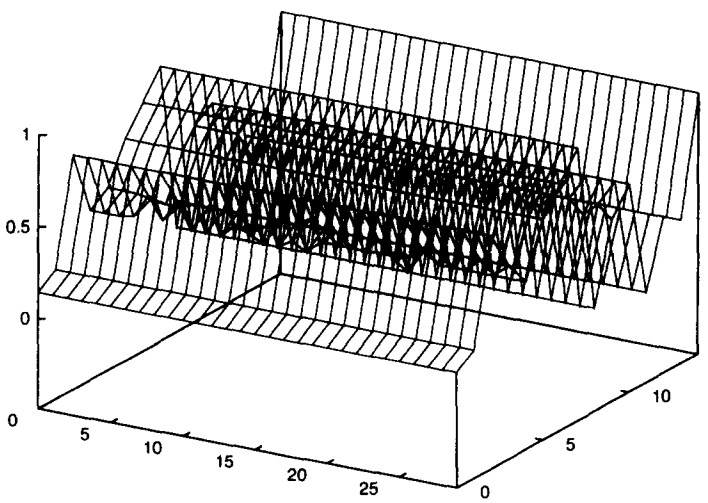

Fig. 1. Time evolution of $\langle P_i \rangle$ for 15 individuals randomly extracted from 50 000 individuals simulated on a 2D lattice whose size is 400×400 ($\rho = N/L \times L$), for $\eta = 5$ and $\mu = 0.1$. The x-axis corresponds to the individuals (numbered from 0 to 14); the y-axis corresponds to time (1 unit = 10^3 time steps: $\langle P_i \rangle$ is recorded every 10^3 time steps, so that time ranges here from 0 to 30×10^3 steps; the first 10^6 steps of the simulation have been discarded); the z-axis represents $\langle P_i \rangle$ (ranges from 0 to 1). Here, $\rho \gg \rho_c \approx 0.1$; individuals rapidly reach their asymptotic $\langle P_i \rangle$; fluctuations are rare.

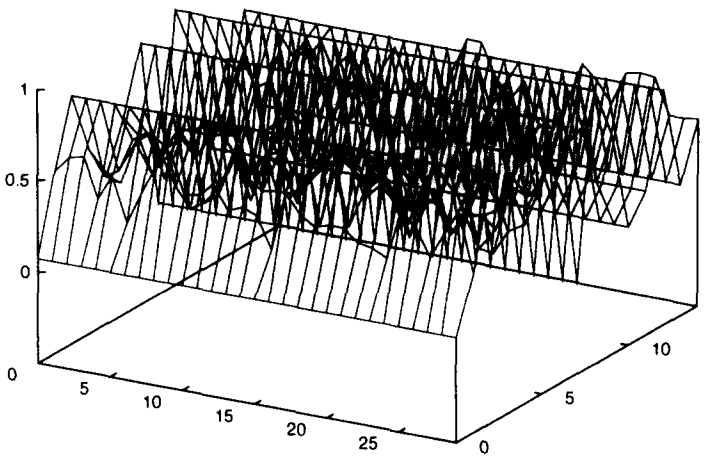

Fig. 2. Same as previous figure for a lattice of size 55×55. The $\langle P_i \rangle$'s begin to undergo important temporal fluctuations, precursor of the supercritical bifurcation.

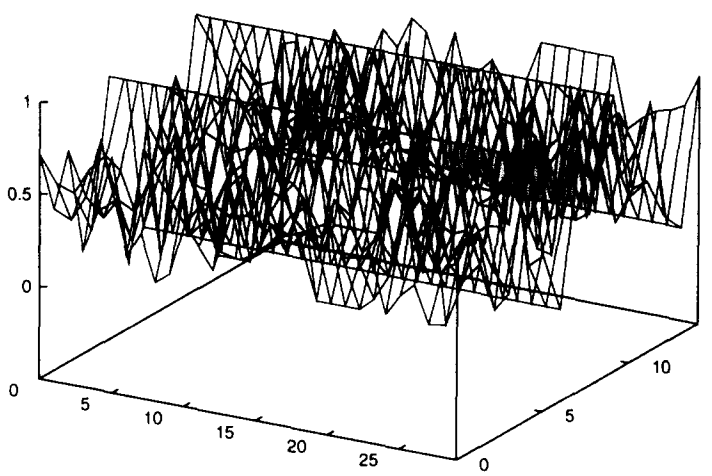

Fig. 3. Same as previous two figures for a lattice of size 70×70. ρ is close to but above its treshold of instability ρ_c. Fluctuations of the $\langle P_i \rangle$'s almost completely destroy the hierarchical structure.

different: this corresponds to the "ordered" or "laminar" phase (see Fig. 1). Figs. 3 and 4 represent intermediate situations, where ρ is close to but above ρ_c: as ρ approaches ρ_c, fluctuations of $\langle P_i \rangle$'s increase, but all $\langle P_i \rangle$'s reach a stable state after a variable amount of time.

The case represented in Figs. 1–4 corresponds to a situation in which the "turbulent" phase is entered smoothly: Figs. 1–3 show that the system exhibits "critical fluctuations" as ρ gets closer to ρ_c. By contrast, for other values of η, fluctuations remain small and the transition from the laminar to the tubulent phase takes place abruptly. One other interesting observation is that the amount of time taken to reach

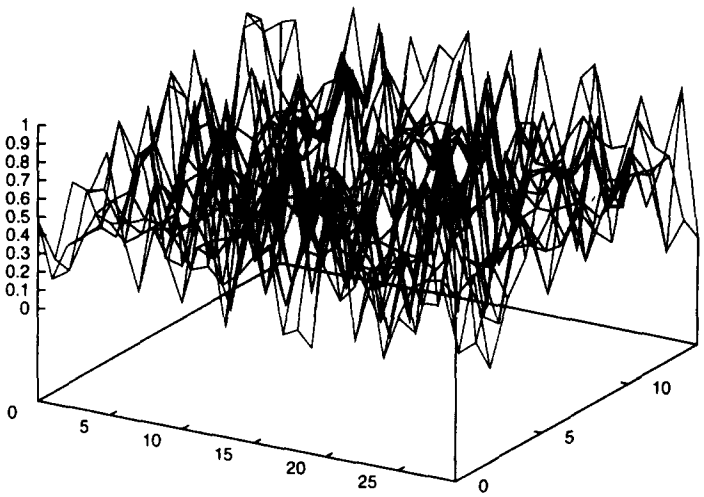

Fig. 4. Same as Figs. 1, 2, and 3, for a lattice of size 100×100. Here, ρ is less than ρ_c. The evolution of the $\langle P_i \rangle$'s is erratic.

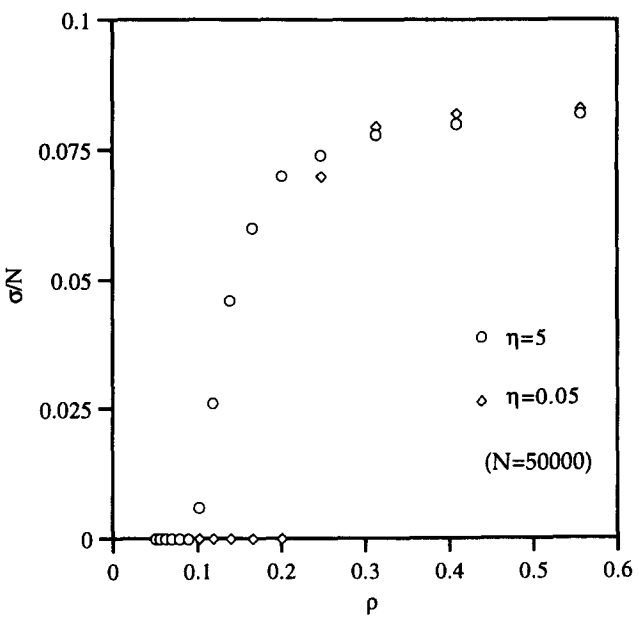

Fig. 5. Value of σ/N vs. ρ ($N = 50\,000$, lattice sizes ranging from 300×300 to 1000×1000) obtained after 10^6 steps from Monte Carlo simulations for $\eta = 5$ (circles), $\eta = 0.05$ (diamonds), and $\mu = 0.1$. The variation of σ/N exhibits no discontinuous jump as ρ crosses ρ_c for $\eta = 5$, while this is the case for $\eta = 0.05$.

the asymptotic state *may or may not diverge* as ρ_c is approached, depending on the value of η. This strongly suggests that there is a crossover from a critical (or supercritical) bifurcation exhibiting critical slowing down to a subcritical bifurcation characterized by a discontinuous jump from a flat to a differentiated hierarchical

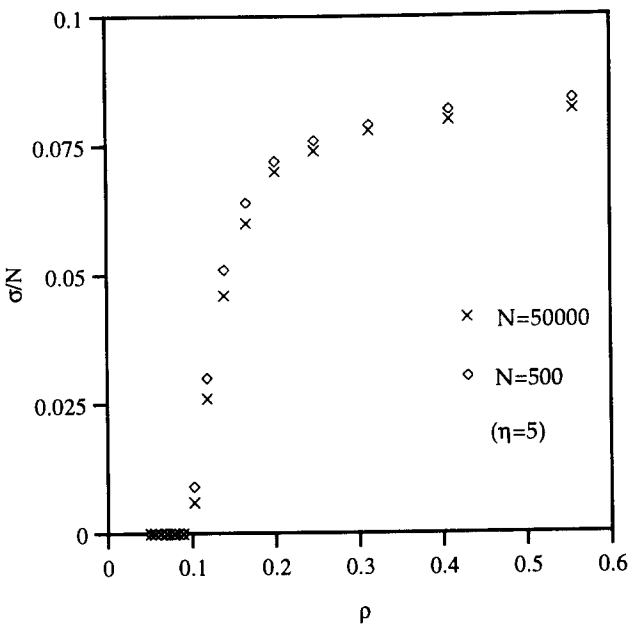

Fig. 6. Value of σ/N vs. ρ obtained after 10^6 steps from Monte Carlo simulations with $\eta = 5$ and $\mu = 0.1$, for two different values of N: $N = 500$ (diamonds) and $N = 50\,000$ (crosses). The variation of σ/N exhibits no discontinuous jump as ρ crosses, ρ_c for $\eta = 5$, while this is the case for $\eta = 0.05$.

profile. This seems to be confirmed from the variance of the hierarchical profile, $\sigma^2 = \sum_{i=0}^{N}(X_i - 0.5)^2$, which can be considered as an order parameter: σ^2 undergoes a smooth transition for $\eta \gg 1$ and an discontinuous transition for $\eta \ll 1$. See Fig. 5, where σ/N ($N = 50\,000$) has been represented as a function of ρ for two values of η: $\eta = 0.005$ and $\eta = 5$. The simulations have been performed for 10^6 time steps (all individuals perform one move within 1 time step) on 2D lattice whose sizes range from 300×300 to 1000×1000. The results do not appear to depend on the size of the system considered: Fig. 6 represents the ρ-dependence of σ/N for $N = 500$ and $N = 50\,000$: the two curves are similar. Finally, if the same simulations are performed with another relaxation rule, such as $F \to F - \mu F$, only continuous transitions are observed. Most of these results can be explained to a large extent with a mean-field theory that we now develop.

3. Mean-field theory

We propose to model the establishment of the hierarchical profile by defining mean-field equations of evolution for the quantities of interest. These equations describe the behaviors of D (dominances), S (subordinations) and F (abstract

force) $= D - S$ for $N + 1$ individuals indexd by $i = 0$ to N:

$$\frac{\mathrm{d}D_i}{\mathrm{d}t} = \frac{\rho}{N} \sum_{\substack{j=0 \text{ to } N \\ j \neq i}} \frac{1}{1 + \mathrm{e}^{-\eta(F_i - F_j)}},$$

$$\frac{\mathrm{d}S_i}{\mathrm{d}t} = \frac{\rho}{N} \sum_{\substack{j=0 \text{ to } N \\ j \neq i}} \frac{1}{1 + \mathrm{e}^{+\eta(F_i - F_j)}}, \tag{2}$$

$$\frac{\mathrm{d}F_i}{\mathrm{d}t} = \frac{\mathrm{d}D_i}{\mathrm{d}t} - \frac{\mathrm{d}S_i}{\mathrm{d}t} - \mu g(F_i),$$

where ρ is the density of individuals, μ is the (constant) decay rate (set to 0.1 in the numerical integrations reported below) and g is a function describing the effect of forgetting. We took $g(F_i) = \tanh(F_i)$, so as to obtain a saturated decay at large values of F, and a decay proportional to F for small F: this choice seems biologically plausible. Eqs. (2) express the fact that each individual, labelled by i, evolves in the mean-field of the other individuals. The force is allowed to take arbitrarily large values. Given the form used for the probabilities of winning and losing, these large values allow for a stabilization of the hierarchical profile. Once again, we expect forgetting to be a crucial parameter, since a small value of ρ/μ certainly prevents the hierarchy from appearing since dominance and subordination events are forgotten between two successive interactions. It is the ratio between the probability of interaction and the forgetting coefficient which is the relevant parameter. In the numerical integration of (2), unless otherwise stated, we used uniform initial conditions: $\forall i$, $D_i = S_i = 1$, and $F_i = 0$. This state being a (sometimes unstable) fixed point of the dynamics, we have supplemented the last equation with a small noise term: any finite amount of noise allows to destabilize (accidental) unstable equilibria. We kept noise to a low enough level in order not to destroy stable asymptotic profiles by too large fluctuations. This addition of noise is simply a convenient alternative to starting from random initial conditions, and does not change the averaged numerical results significantly. For a discussion about the effect of noise on bifurcations in dynamical systems, see e.g. Ref. [17] and references therein. The theoretical discussions will be made on the deterministic system. In conclusion, our mean-field approach is essentially deterministic. The noise term added in the numerical integration is taken to be gaussian, centered, of variance θ and uncorrelated in space and time:

$$\forall i,j,t,t' \qquad \langle \xi(i,t) \rangle = 0 \text{ and } \langle \xi(i,t)\, \xi(j,t') \rangle = \theta^2 \delta(i-j)\, \delta(t-t'), \tag{3}$$

where δ is the Dirac function.

We have integrated the Langevin equations (2) and (3) numerically with Stratanovitch interpretation for 10 individuals, because it is a typical number for colonies of wasps *Polistes*. Other animal societies comprising a larger number of individuals exhibit non-trivial hierarchical structures: this is the case for instance of some bumble bees, whose colonies may contain about 40 individuals or more [14]. Numerical tests carried out on such larger populations (up to 5000: the computational cost becomes

phohibitive above this number, since the number of calculations per time step is of the order of N^2) show that the same hierarchical profiles and the same properties are obtained, yet on a larger scale.

In the absence of forgetting (i.e. $\mu = 0$), we obtain a profile linear in X (X_i as a function of the rank of individual i), consistent with the one found in Monte Carlo simulations reported in [18]. It can be shown that the linear dependence of X_i with respect to the rank is an asymptotic stationary state (in X_i). In effect, X_i and F_i can be simply related by $F_i/\rho t = 2X_i - 1$, since $F_i = D_i - S_i$ (there is a rate ρ of interaction per time step for every individual, so that $D_i + S_i = \rho t$) and $X_i = D_i/D_i + S_i$. Therefore, a time-independent linear variation of X_i as a function of rank should result in $F_{i_{t\to\infty}} = \rho k_i t$, where k_i is a time-independent quantity. Under very general conditions, assuming that individuals are numbered according to their ranks, the only asymptotically stationary profile is given by $k_0 = -1, \ldots, k_i = -1 + 2i/N, \ldots, k_N = 1$, i.e. a profile linear in the rank i. To see this, let us assume that we have $F_{i_{t\to\infty}} = \rho k_i t$, and that the k_i's satisfy strict inequalities: $k_0 < k_1 < \cdots < k_j < \cdots < k_N$. We can inject this form for F_i in the equation giving the evolution of F_i (in the absense of noise):

$$\frac{\mathrm{d}F_i}{\mathrm{d}t} = \frac{\rho}{N} \sum_{\substack{j=0 \text{ to } N \\ j \neq i}} \left(\frac{1}{1 + \mathrm{e}^{-\rho t(k_i - k_j)}} - \frac{1}{1 + \mathrm{e}^{+\rho t(k_i - k_j)}} \right). \tag{4}$$

As $t \to \infty$, $1/(1 + \mathrm{e}^{-\rho t(k_i - k_j)}) \to 0$ (resp. 1) and $1/(1 + \mathrm{e}^{-\rho t(k_i - k_j)}) \to 1$ (resp. 0) if $j > i$ (resp. $j < i$). Consequently, there are i terms equal to 1 and $N - i$ terms equal to -1 in the sum, so that finally

$$\frac{1}{N} \sum_{\substack{j=0 \text{ to } N \\ j \neq i}} \left(\frac{1}{1 + \mathrm{e}^{-\rho t(k_i - k_j)}} - \frac{1}{1 + \mathrm{e}^{+\rho t(k_i - k_j)}} \right)_{t\to\infty} = -1 + \frac{2i}{N}, \tag{5}$$

which corresponds to the linearly varying profile $k_i = -1 + 2i/N$, obviously consistent with the condition $k_0 < k_1 < \cdots < k_i < \cdots < k_N$. Simulations confirm that this state is an effective attractor of the hierarchy formation dynamics.

As expected, the inclusion of forgetting leads to new phenomena which are qualitatively different depending on the value of η. To summarize, a bifurcation is always observed as the population density ρ is increased from 0 to 1. The bifurcation takes place at $\rho = 2\mu/[\eta(1 + 1/N)]$: for $\rho < 2\mu/[\eta(1 + 1/N)]$, there is no hierarchical differentiation, i.e. the profile is flat, while for $\rho > 2\mu/[\eta(1 + 1/N)]$ the asymptotic profile corresponds to a developed hierarchy. When $\eta < 2/(1 + 1/N)$, the bifurcation is subcritical (or discontinuous: see Fig. 7, where the "order parameter" is simply the variance of the profile $\sigma^2 = \sum_{i=0}^{N}(X_i - 0.5)^2$), provided initial conditions are not too disordered, and when $\eta \geqslant 2/(1 + 1/N)$, the bifurcation is critical (or continuous: see Fig. 8), exhibits critical slowing down and can be characterized by critical exponents. Fig. 9 shows that the transition is "more discontinuous" for smaller values of η. Fig. 10 is identical to Fig. 8 with $\mu = 5$.

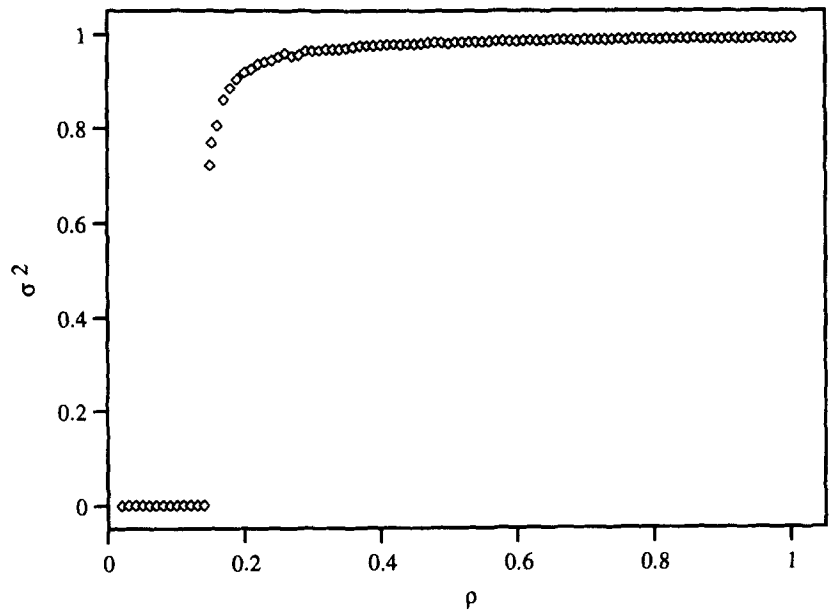

Fig. 7. Order parameter σ^2 as a function of ρ for $\eta = 1.5$, obtained from numerical integration of Eqs. (2) and (3), $N = 10$.

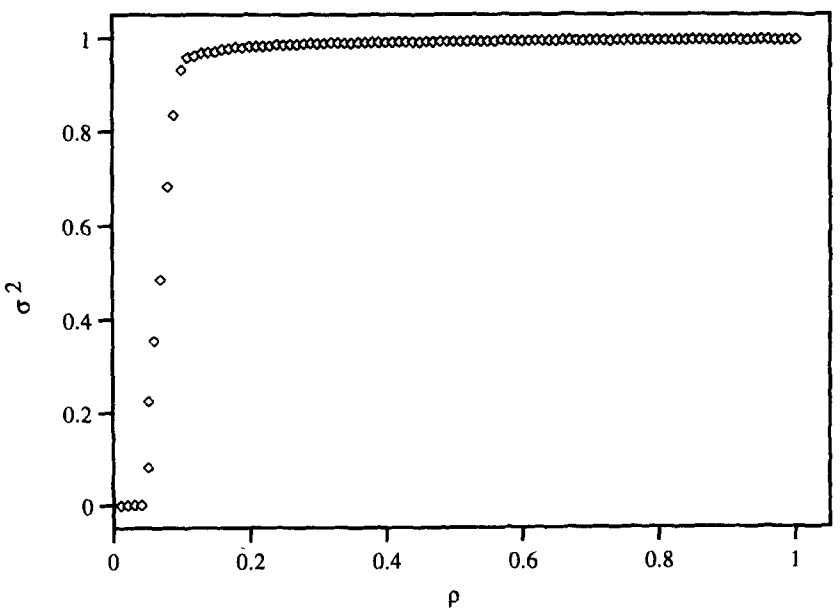

Fig. 8. Same as Fig. 7 for $\eta = 4$.

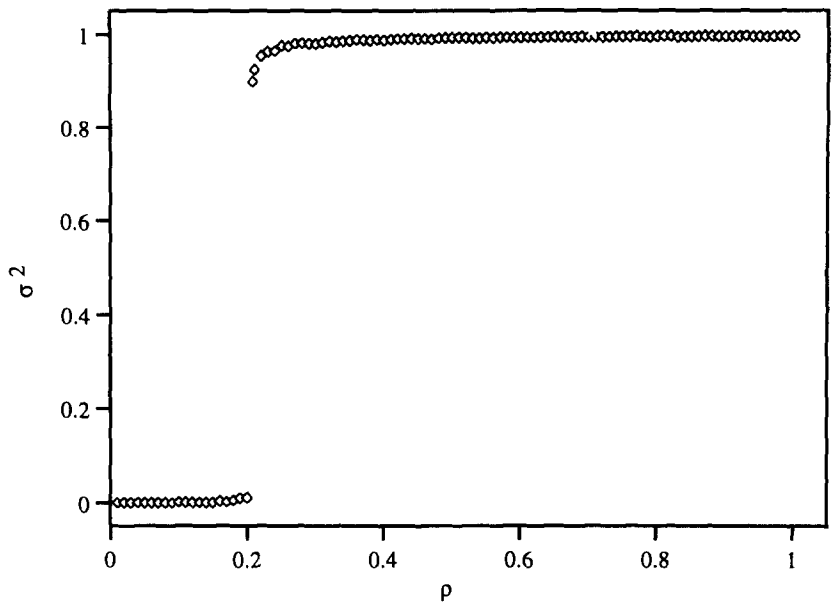

Fig. 9. Same as Fig. 7 for $\eta = 1$.

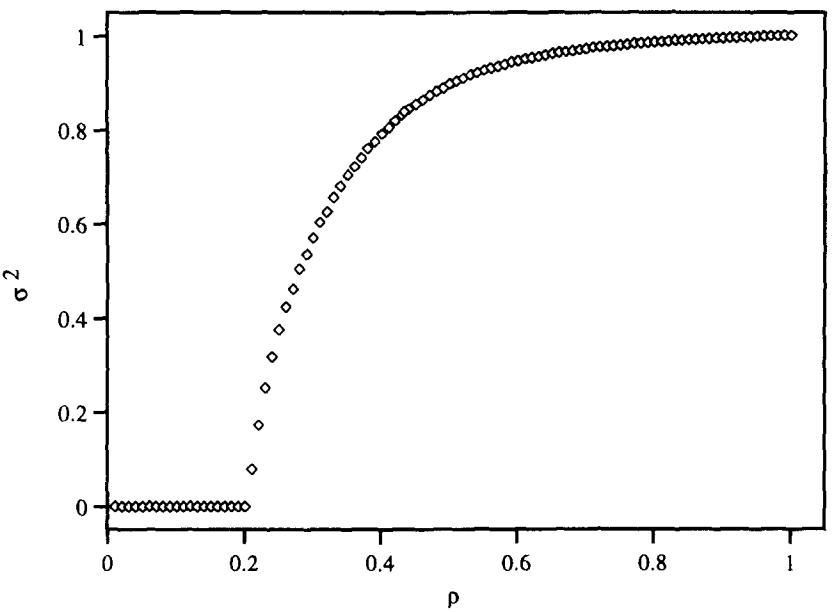

Fig. 10. Same as Fig. 7 for $\mu = 0.5$, $\eta = 5$.

In the case $\eta < 2/(1 + 1/N)$, it is easy to show that there are many coexisting stable states, but the undifferentiated state (flat profile) is linearly stable and has a wide basin of attraction. Linear stability does not imply stability under macroscopic perturbations, so that strong enough fluctuations or perturbations (either in the dynamics or in the boundary conditions) can make the hierarchy appear, even for $\rho < 2\mu/[\eta(1 + 1/N)$. Simulations show that such perturbations must indeed be very strong to destabilize the non-hierarchical behavior when $\eta \ll 2/(1 + 1/N)$: if the system starts with initial conditions close enough to the flat profile, the transition therefore gives the impession of being discontinuous; at the bifurcation point, there is an abrupt change in the profile due to the coexistence of other stable states (Fig. 11). As one approaches $\eta = 2/(1 + 1/N)$ from below, the stability of the flat profile is more and more local and can be destroyed with smaller and smaller fluctuations. This relative stability of the flat profile with respect to perturbations may explain some differences between the mean-field approach and the Monte Carlo simulations. In particular, we observe that for small values of η, the mean-field critical density ρ_c^{MF} and the Monte Carlo critical density ρ_c^{MC} satisfy $\rho_c^{MC} \leqslant \rho_c^{MF}$: the random encounters in the Monte Carlo simulations induce fluctuations allowing the system to settle in other stable states for smaller values of the density than in the mean-field case.

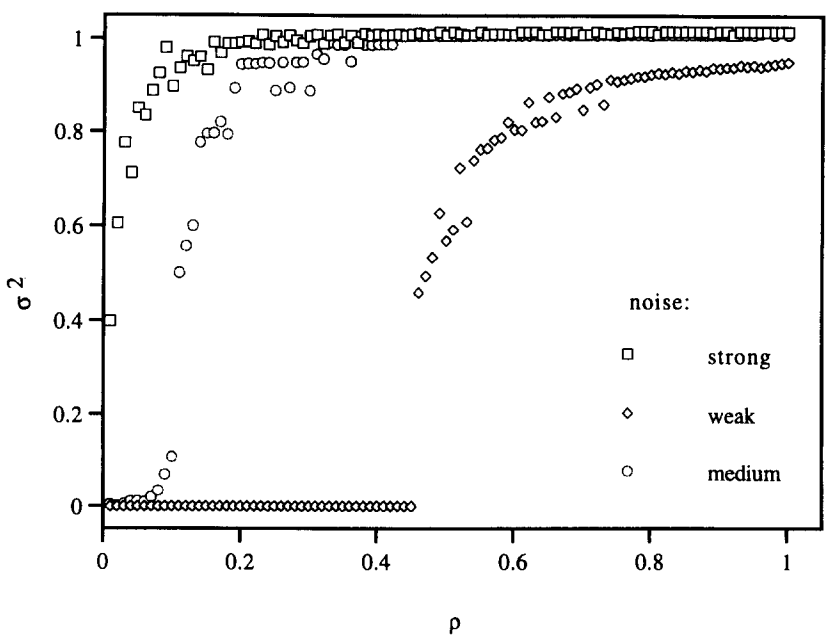

Fig. 11. Effects of the strength of perturbations on the bifurcation and the stable states for $\eta = 0.5$, $\mu = 0.1$, $N = 10$. Strong noise means that initial conditions for F were chosen to be uniformly distributed in $[-500, +500]$, in $[-50, +50]$ for medium noise, and in $[-5, +5]$ for weak noise. The effects would be similar with different levels of noise in the dynamics itself (instead of initial conditions).

In contrast, when $\eta \geqslant 2/((1 + 1/N)$, the transition is smooth because there is only one single stable state in the low density region: the flat profile. This stable state becomes unstable at the transition point which also corresponds to the appearance of new stable states (which did not exist below the critical density). Such a destabilizing process is typical of critical phase transitions in physics.

4. Analysis for two individuals ($N = 1$)

In the case where there are 2 individuals, an equation similar to (1) can easily be derived. We start with the two deterministic equations for the two forces:

$$\begin{aligned}\frac{dF_1}{dt} &= \frac{\rho}{N}\left(\frac{1}{1+e^{-\eta(F_1-F_2)}} - \frac{1}{1+e^{+\eta(F_1-F_2)}}\right) - \mu\tanh(F_1),\\ \frac{dF_2}{dt} &= \frac{\rho}{N}\left(\frac{1}{1+e^{+\eta(F_1-F_2)}} - \frac{1}{1+e^{-\eta(F_1-F_2)}}\right) - \mu\tanh(F_2),\end{aligned} \tag{6}$$

Let us introduce $\Delta = F_1 - F_2$ and $\Gamma = F_1 + F_2$. The evolution equations for Δ (the simplest order parameter here) and Γ read:

$$\begin{aligned}\frac{d\Delta}{dt} &= H(\Delta) = 2\rho\left(\frac{1}{1+e^{-\eta\Delta}} - \frac{1}{1+e^{+\eta\Delta}}\right) - 2\mu\frac{\mathrm{sh}\Delta}{\mathrm{ch}\Delta + \mathrm{ch}\Gamma},\\ \frac{d\Gamma}{dt} &= -2\mu\frac{\mathrm{sh}\Gamma}{\mathrm{ch}\Delta + \mathrm{ch}\Gamma}.\end{aligned} \tag{7}$$

(Remember that for two individuals $N = 1$.) Given the particular form of the second equation, the first one can be approximated by

$$\frac{d\Delta}{dt} = H(\Delta) = 2\rho\left(\frac{1}{1+e^{-\eta\Delta}} - \frac{1}{1+e^{+\eta\Delta}}\right) - 2\mu\frac{\mathrm{sh}\Delta}{\mathrm{ch}\Delta + 1}. \tag{8}$$

Looking for the temporal evolution of Δ in the vicinity of $\Delta = 0$, we may expand $H(\Delta)$ around $\Delta = 0$ so that (8) is transformed into

$$\begin{aligned}\frac{d\Delta}{dt} &= H(0) + \Delta H'(0) + \tfrac{1}{2}\Delta^2 H''(0) + \tfrac{1}{6}\Delta^3 H'''(0) + \tfrac{1}{24}\Delta^4 H^{(4)}(0)\\ &\quad + \tfrac{1}{120}\Delta^5 H^{(5)}(0) + \cdots\\ &= (\eta\rho - \mu)\Delta - 2(\tfrac{1}{4}\eta^3\rho - \tfrac{1}{4}\mu\tfrac{1}{6}\Delta^3 + \cdots.\end{aligned} \tag{9}$$

Injecting the value of the critical value of $\rho = \mu/\eta$ into the coefficient of the Δ^3 term, we get Eq. (1) with $\alpha = \frac{1}{12}\mu(\eta^2 - 1)$. As expected, we have a crossover from a subcritical to a critical bifurcation at $\eta = 2/(1 + 1/N) = 1$: the bifurcation is subcritical (resp. supercritical) for $\eta < 1$ (resp. $\eta > 1$). Note that the bifurcation is always supercritical if the relaxation function for F is $g(F_i) = F_i$, supporting the observation made in the

Monte Carlo simulations. In effect, expression (9) has then to be replaced by $\mathrm{d}\Delta/\mathrm{d}t = (\eta\rho - \mu)\Delta - \frac{1}{12}\eta^3\rho\Delta^3 + \cdots$.

5. Analysis for $N > 1$

For larger values of N, the previous observations can be understood in two steps: (1) stability analysis of the flat profile (similar to the case of two individuals); (2) "physical" constraints imposed on the profile. The latter treatment allows to avoid the complete calculation of the multivariate higher-order derivatives necessary to obtain Eq. (1).

5.1. Stability analysis

Let us study the last equation of (2):

$$\frac{\mathrm{d}F_i}{\mathrm{d}t} = H_i(\{F_j\}) = \frac{\rho}{N}\left(\sum_{\substack{j=0 \text{ to } N \\ j\neq i}} \frac{1}{1+\mathrm{e}^{-\eta(F_i-F_j)}} - \frac{1}{1+\mathrm{e}^{+\eta(F_i-F_j)}}\right) - \mu g(F_i). \tag{10}$$

The associated Jacobian matrix $[\partial H_i/\partial F_j]$ is defined by:

$$\frac{\partial H_i}{\partial F_i} = \frac{\rho}{N}\left(\sum_{\substack{j=0 \text{ to } N \\ j\neq i}} \frac{\eta\mathrm{e}^{-\eta(F_i-F_j)}}{(1+\mathrm{e}^{-\eta(F_i-F_j)})^2} + \frac{\eta\mathrm{e}^{-\eta(F_i-F_j)}}{(1+\mathrm{e}^{+\eta(F_i-F_j)})^2}\right) - \mu\frac{\mathrm{d}g}{\mathrm{d}F}(F_i),$$

$$\left.\frac{\partial H_i}{\partial F_j}\right|_{i\neq j} = -\frac{\rho}{N}\left(\frac{\eta\mathrm{e}^{-\eta(F_i-F_j)}}{(1+\mathrm{e}^{-\eta(F_i-F_j)})^2} + \frac{\eta\mathrm{e}^{-\eta(F_i-F_j)}}{(1+\mathrm{e}^{+\eta(F_i-F_j)})^2}\right). \tag{11}$$

The stability of a state such that $F_0 = F_2 = \cdots = F_N = F$ is determined by the eigenvalues of

$$[\partial H_i/\partial F_j|_{F_0=F_2=\cdots=F_N=F}] = \begin{bmatrix} \rho\frac{\eta}{2} - \frac{\mathrm{d}g}{\mathrm{d}F} & -\frac{\rho}{N}\frac{\eta}{2} & \cdots & \cdots & -\frac{\rho}{N}\frac{\eta}{2} \\ -\frac{\rho}{N}\frac{\eta}{2} & \ddots & -\frac{\rho}{N}\frac{\eta}{2} & \ddots & \vdots \\ \vdots & -\frac{\rho}{N}\frac{\eta}{2} & \ddots & -\frac{\rho}{N}\frac{\eta}{2} & \vdots \\ \vdots & \ddots & -\frac{\rho}{N}\frac{\eta}{2} & \ddots & -\frac{\rho}{N}\frac{\eta}{2} \\ -\frac{\rho}{N}\frac{\eta}{2} & \cdots & \cdots & -\frac{\rho}{N}\frac{\eta}{2} & \rho\frac{\eta}{2} - \frac{\mathrm{d}g}{\mathrm{d}F} \end{bmatrix}, \tag{12}$$

which is a circulating matrix. The state $F_0 = F_2 = \cdots = F_N = F$ is therefore stable for

$$\rho < 2\mu\frac{\mathrm{d}g}{\mathrm{d}F}\Big/\left[\eta\left(1+\frac{1}{N}\right)\right]. \tag{13}$$

Since $dg/dF \to 0$ as F increases, the most stable state of this kind is when $F = 0$. The stability condition is then given by

$$\rho < 2\mu \Big/ \left[\eta\left(1 + \frac{1}{N}\right)\right]. \tag{14}$$

if $dg/dF|_{F=0} = 0$, which is indeed satisfied in the studied case. To summarize, the flat profile is linearly stable for $\rho < 2\mu/[\eta(1 + 1/N)]$ and linearly unstable for $\rho > 2\mu/[\eta(1 + 1/N)]$.

5.2. *Allowed profiles*

The stability analysis is not sufficient. In particular, there are structural constraints imposed on the profiles. If the constraints are not satisfied ($\rho < \mu$), slightly differentiated profiles may appear in the region where the flat profile is linearly unstable, but these profiles are local attractors, and two runs of the process lead to two different profiles. On the contrary, if the constraints are satisfied ($\rho > \mu$), one particular profile is a global attractor, and two runs converge to the same profile. Note that a profile is anonymous: it is a function that associates a dominance index to a rank; therefore two equivalent profiles may correspond to situations where individuals are in different situations (the hierarchical symmetry between individuals is broken). One then understands that the nature of the transition from a flat to a differentiated situation depends on the relative locations of the linear unstability point and the point where the constraints become satisfied, i.e. $2\mu/[\eta(1 + 1/N)]$ and μ. To understand the nature of these constraints, we follow the same line of reasoning as in the case without forgetting, but now including the forgetting term: the corresponding deterministic equations read

$$\frac{dF_i}{dt} = \rho \frac{d}{dt}[t(2X_i - 1)] - \mu g(F_i). \tag{15}$$

From the previous discussion, it is reasonable to start by assuming that $dF_i/dt \underset{t\to\infty}{=} \rho k_i$. Looking for a stationary solution for X_i, we get the following equations:

$$-1 + 2i/N - \mu g(\rho k_i t) = \rho(2X_i - 1). \tag{16}$$

If $g(F_i) = \tanh(F_i)$, (16) can be approximated by $-1 + 2i/N - \mu \operatorname{sign}(k_i) = \rho(2X_i - 1)$, i.e.

$$\begin{aligned} X_i &= \frac{i}{N} + \frac{\mu}{2\rho} \quad \text{if } k_i < 0, \\ X_i &= \frac{i}{N} - \frac{\mu}{2\rho} \quad \text{if } k_i > 0. \end{aligned} \tag{17}$$

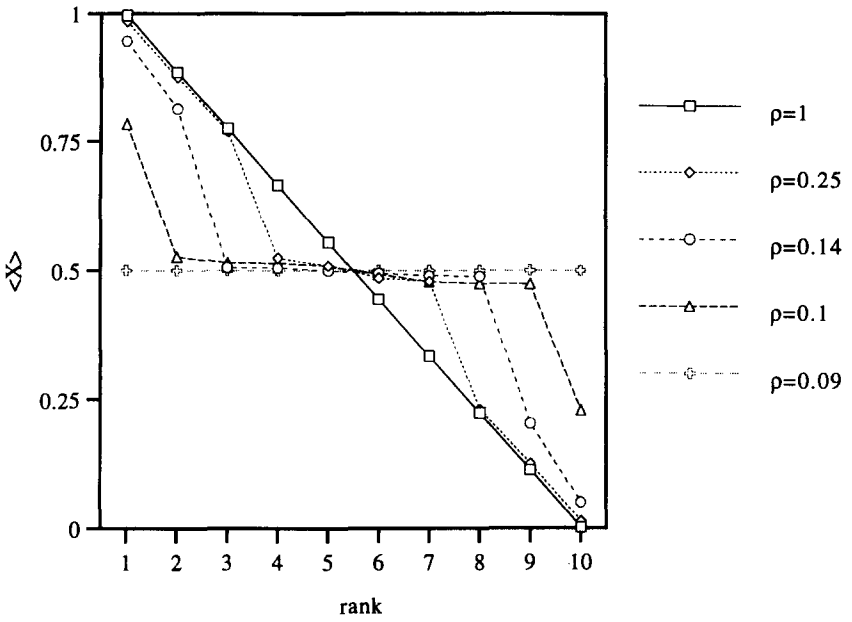

Fig. 12. Asymptotic profile for various values of ρ at $\eta = 2$, $\mu = 0.1$, $N = 10$.

This set of equations (17) has a solution, with some of the $X_i \neq 0.5$ (i.e. a differentiated profile) if and only if the following set of consistency conditions are satisfied: $i/N_{i=0} + \mu/2\rho < \frac{1}{2}$ and $i/N_{i=N} - \mu/2\rho < \frac{1}{2}$, which both reduce to

$$\rho > \mu. \tag{18}$$

Therefore the profile should in principle be completely flat below $\rho_c = \mu$. To be more accurate, for $\rho > \rho_c$, the profile is expected to be flat between two values of i, symmetric with respect to $i = N/2$, $i_{\text{inf}}(\rho) = N/2 - N\mu/2\rho$ and $i_{\text{sup}}(\rho) = N/2 + N\mu/2\rho$, and to vary linearly from $i = 0$ to i_{inf}, and from i_{sup} to N. This is indeed observed for $\eta = 2/(1 + 1/N)$ (see Fig. 12). For other values of η, the situation is different:

(1) If $\rho > \mu$ but the flat profile is still linearly stable (this is the case when $\eta < 2/(1 + 1/N)$), small fluctuatios will not suffice to make the hierarchy appear, but as soon as the flat profile is unstable, the hierarchy emerges abruptly, defined by Eqs. (17).

(2) If $\rho < \mu$ and the flat profile is linearly unstable (this happens when $\eta > 2/(1 + 1/N)$, the hierarchy appears – because the flat profile cannot persist – but not in a structured way: the profiles look more or less random. This is due to the fact that the profile is entirely the effect of fluctuations, since condition (18) is not fulfilled.

(3) When $\eta = 2/(1 + 1/N)$, condition (18) becomes satisfied exactly at the time when the flat profile becomes linearly unstable (i.e. at $2\mu/[\eta(1 + 1/N)]$). A tricritical point will always be obtained for $\eta = 2/(1 + 1/N)$; only the corresponding critical value of ρ varies as $2\mu/[\eta(1 + 1/N)]$.

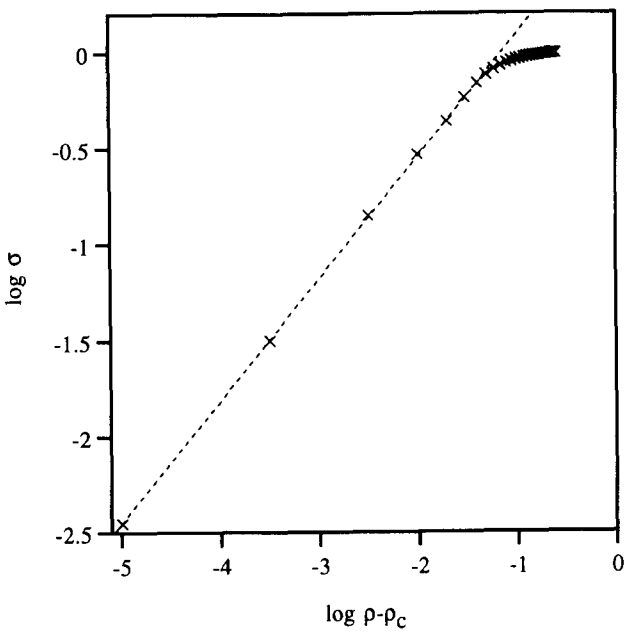

Fig. 13. Log σ vs. $\log(\rho - \rho_c)$, $\eta = 2$, $\mu = 0.1$, $N = 10$. The slope of the straight line yields $\alpha = 0.625 \pm 0.005$. This curve has been obtained by averaging over 20 simulations for each value of ρ.

Note that the critical case, $\eta \geqslant 2/(1 + 1/N)$, can be characterized by critical exponents. In the vicinity of the transition, the order parameter follows $\sigma \propto (\rho - \rho_c)^{\alpha}$, where the exponent α seems to depend on the particular values of μ and η, but not on N. For example, Fig. 13 represents $\log \sigma$ vs. $\log(\rho - \rho_c)$ for $\eta = 2$, $N = 10$, $\mu = 0.1$; the exponent is $\alpha = 0.625 \pm 0.005$. Moreover, one also observes a divergence of the time scale over which the hierarchical profile is formed. In order to determine the timescale T_s necessary for the hierarchy to get established, we define a criterion based on an arbitrary but reasonable, empirically determined threshold φ: when the order parameter, i.e. the excursion of the profile around the flat profile, exceeds a certain value φ (i.e when $\sigma^2 \geqslant \varphi$), it becomes amplified, and the hierarchy is eventually established in its stable form if one waits long enough. Of course, the value ρ_{T_s} of ρ at which T_s diverges depends on φ: $\rho_{T_s(\varphi)} \underset{\varphi \to 0}{\to} \rho_c$. Then T_s varies as $T_s \propto (\rho - \rho_c)^{-\zeta}$, where ζ is a characteristic dynamical exponent illustrating the critical slowing down of the process. For example, for $\eta = 2$ and $\mu = 0.1$, $\zeta = 1.39 \pm 0.1$ (see Fig. 14). Finally, as already mentioned, there is also an associated broken symmetry: when the density is insufficient, individuals are all equivalent, and all have a time-averaged value of X_i equal to 0.5. When $\rho > \rho_c$, however, individuals are not equivalent: a hierarchy is determined not only by the hierarchical profile, but also by the respective ranks of all individuals; if the profile is flat, both informations are equivalent, but when there is a differentiation, it is not sufficient to know the profile to determine the rank of an individual. Therefore, one non-flat profile corresponds to $N!$ combinations $(i, \text{rank}(i))$: the system settles in one of these permutations, breaking the symmetry between

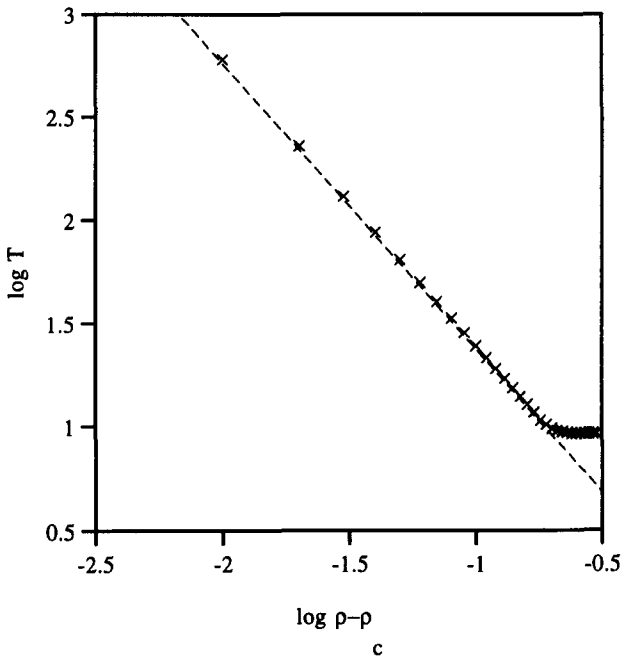

Fig. 14. Log($T_s(\rho)$) vs. log($\rho - \rho_c$) for a fixed, low value of φ (= 0.0001), $\eta = 2$, $\mu = 0.1$, $N = 10$. The slope of the straight line gives the dynamical exponent $\zeta = 1.39 \pm 0.1$. This curve has been obtained by averaging over 20 simulations for each value of ρ.

individuals. We guess that it is the role of any hierarchy to break the symmetry between individuals.

6. Conclusion

We have introduced a simple model of how a hierarchical profile may emerge in a population of anonymous organisms, i.e. involving no individual recognition, and shown that there is a bifurcation as the density of individuals is tuned. We showed that the lower the density, the weaker the hierarchical differentiation, whose level is measured by the ad hoc order parameter $\sigma^2 = \sum_{i=0}^{N}(X_i - 0.5)^2$. The nature of the bifurcation – super- or subcritical – has been shown within a mean-field approach to depend on the value of the temperature-like parameter which describes the amount of determinism in the outcome of a fight. The supercritical bifurcations are characterized by critical exponents, and critical slowing down. The subcritical bifurcations, more difficult to characterize due to the absence of a small parameter, correspond to a higher linear stability of the flat profile, and the presence of coexisting stable states, which are macroscopically far from the flat profile. The results are summarized in the phase diagram represented in Fig. 15. Our system is a globally coupled system whose transition to non-hierarchical behavior is very reminiscent of a (possibly intermittent)

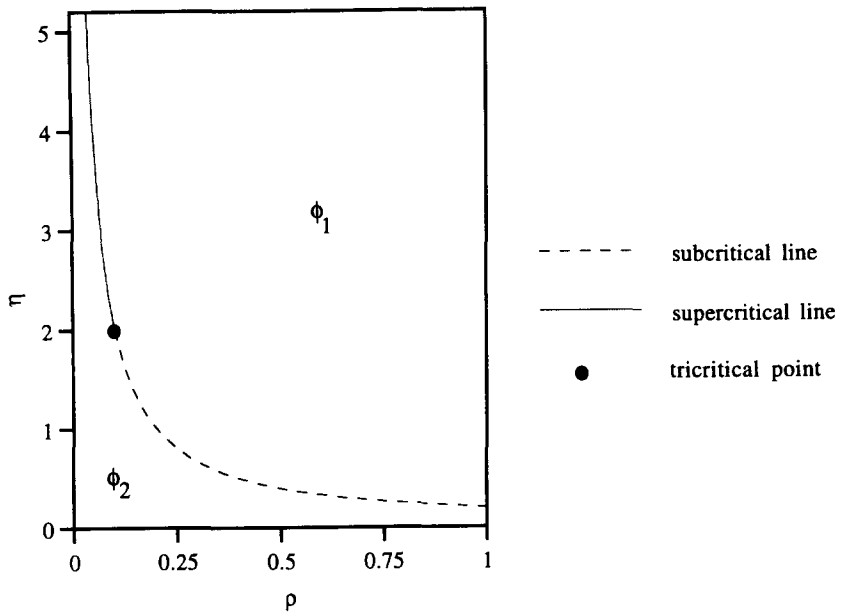

Fig. 15. Mean-field phase diagram of the model. ϕ_1 is the (dynamically) ordered phase, i.e. with a hierarchical differentiation, and ϕ_2 is the (dynamically) disordered phase, i.e. corresponding to flat hierarchical profiles. We observe a line of supercritical bifurcations for $\eta \geqslant 2/(1 + 1/N)$ and a line of subcritical (discontinuous) bifurcations for $\eta < 2/(1 + 1/N)$. $\eta = 2/(1 + 1/N)$ corresponds to a tricritical point.

transition to turbulence in coupled-map lattices (see e.g. [19]). Chaté and Manneville [20] have indeed also observed transitions to turbulence in coupled-map lattices as a coupling parameter is varied (this coupling parameter can be paralleled with our coupling parameter ρ): the nature of these transitions – continuous or discontinuous – were shown to depend on the parameters of the local map (embodied by η in our model). For continuous transitions, the critical exponents did also depend on the particular details of the local map. As regards universality classes, the "laminar" state not being absorbing in the present model, the question of whether it belongs to the RFT class (directed percolation) is irrelevant. The notion of out-of-equilibrium universality classes is of course a challenging question.

From the biological viewpoint, in order to test the model used here in the laboratory, it is easy to vary artificially the density of individuals but more difficult to modify the amount of determinism in the outcomes of the fights (this latter parameter can however be evaluated). Experimental and field data suggest that both critical and subcritical bifurcations exist in nature and the present study, based on a physical approach to the problem, indicates what parameters the nature of the transition may depend on: in this respect, it allows the model to be tested experimentally.

References

[1] A. Aitta, G. Ahlers and D.S. Cannell, Phys. Rev. Lett. 54 (1985) 673.
[2] D. Liu, L.M. Williams and H.Z. Cummins, Phys. Rev. E 50 (1994) R4286.
[3] B. Caroli, C. Caroli and B. Roulet, J. Phys. (Paris) 43 (1982) 1767,
G.J. Merchant and S.H. Davis, Phys. Rev. Lett. 63 (1989) 573; Phys. Rev. B 40 (1989) 11140;
D.J. Wollkind and L.A. Segel, Phil. Trans. R. Soc. A 268, (1970) 351.
[4] A.P. Bergé, Y. Pomeau and C. Vidal, Order Within Chaos (Wiley, New York, 1984).
[5] D. Sornette, F. Ferré and E. Papiernik, Int. J. Bifurc. Chaos 4 (1994) 693.
[6] M. Millonas, J. Theor. Biol. 159 (1992) 529.
[7] H.G. Landau, Bull. Math. Biophys. 13 (1951) 1–19;
I. Chase, Behav. Sci. 19 (1974) 374–382.
[8] W.C. Allee, Biol. Symp. 8 (1942) 139–162; Coll. Int. CNRS 34 (1952) 157–181;
A.M. Guhl, Anim. Behav. 16 (1968) 219–232.
[9] M.W. Schein, and M.H. Forman, Brit. J. Anim. Behav. 3 (1955) 45–55.
[10] S.J. Tyler, Anim. Behav. Monogr. 48 (1972) 223–233.
[11] L. Pardi, Boll. Ist. Entom. Univ. Bologna 15 (1946) 25–84; Physiol. Zool. 21 (1948) 1–13.
[12] J. Gerve, Ins. Soc. 9 (1962) 231–263; Ann. Sci. Nat. Zool. 6 (1964) 601–778;
E.O. Wilson, The Insect Societies (1971) Cambridge, Harvard, MA., Belknap Press;
G. Theraulaz, J. Gervet, B. Thon, M. Pratte and S. Semenoff-Tian-Chansky, Ethology 91 (1992) 177–202;
G. Theraulaz, M. Pratte and J. Gervet. Behaviour 113 (1990) 223–250; Actes Coll. Ins. Soc. 5 (1989) 169–179; G. Theraulaz, J. Gerve and S. Semenoff-Tian-Chansky, Behaviour 116 (1991) 292–320.
[13] B.J. Cole, Science 212 (1981) 83–84;
N.R. Franks and E. Scovell, Nature 304 (1983) 724–725;
A.F.G. Bourke, Behav. Ecol. Sociobiol. 23 (1988) 323–333;
P.S. Oliveira and B. Hölldobler, Behav. Ecol. Sociobiol. 27 (1990) 385–393.
[14] C. Van Honk and P. Hogeweg, Behav. Ecol. Sociobiol. 9 (1981) 111–119;
P. Hogeweg and B. Hesper, Behav. Ecol. Sociobiol. 12 (1983) 271–283.
[15] P.-F. Röseler, I. Röseler, A. Strambi and R. Augier, Ecol. Sociobiol. 15 (1984) 133–142;
P.-F. Röseler, Reproductive competition during colony establishment, in: The Social Biology of Wasps, eds. K.G. Ross and R.W. Matthews, pp. 309–335, Comstock Publishing Associates/Cornell University Press, Ithaca, NY, (1991) pp. 309–335.
[16] L.A. Dugatkin, M.S. Alfieri and A.J. Moore, Ethology 97 (1994) 94102.
[17] M.C. Cross and P.C. Hohenberg, Rev. Mod. Phys. 65 (1993) 851.
[18] G. Theraulaz, E. Bonabeau and J.L. Deneubourg, Self-organization of hierarchies in animal societies: the case of the primitively eusocial wasp *Polistes dominulus* Christ., to appear in J. Theor. Biol. (1995).
[19] K. Kaneko, ed., Theory and Applications of Coupled Map Lattices (John Wiley and Sons, Chichester, 1993).
[20] H. Chaté and P. Manneville, Physica D 32 (1988) 409; Europhys. Lett. 6 (1988) 591.